Model Predictive MRAS Estimator for Sensorless Induction Motor Drives

Yaman B. Zbede, Shady M. Gadoue and David J. Atkinson

Abstract—**This paper presents a novel predictive model reference adaptive system (MRAS) speed estimator for sensorless induction motor drives applications. The proposed estimator is based on the finite control set-model predictive control principle. The rotor position is calculated using a search-based optimization algorithm which ensures a minimum speed tuning error signal at each sampling period. This eliminates the need for a PI controller which is conventionally employed in the adaption mechanism of MRAS estimators. Extensive experimental tests have been carried out to evaluate the performance of the proposed estimator using a 2.2kW induction motor with a field oriented control (FOC) scheme employed as the motor control strategy. Experimental results show improved performance of the MRAS scheme in both open and closed-loop sensorless modes of operation at low speeds and with different loading conditions including regeneration. The proposed scheme also improves the system robustness against motor parameter variations and increases the maximum bandwidth of the speed loop controller.**

Index Terms—**Model reference adaptive control, predictive control, induction motor drive, vector control, position estimation, speed estimation.**

I. Introduction

NOWADAYS, Field Oriented Control (FOC) of Induction Motors (IM) has established an increasing popularity in a wide range of applications and acceptance in the electric drives markets worldwide [1]. Over the last two decades, significant efforts have been made in AC drives to eliminate the speed sensor mounted on the machine shaft. This means that the machine speed is estimated rather than measured and this technology is referred to as sensorless control [2]. Although sensorless control has been successfully applied in medium and high speed operating regions, operation at very low speeds still remains a significant problem for IM drives [3].

In sensorless IM drives, a number of techniques have been introduced for speed estimation that vary from open loop to artificial intelligence-based estimators [2]. Among these techniques, Model Reference Adaptive Systems-based (MRAS) estimators have gained great popularity because of their relative simplicity and ease of application [4]. Rotor flux based MRAS has been extensively studied and it has been demonstrated that these estimators can have an excellent performance down to 5% of rated speed [2, 5, 6]. However, rotor flux based MRAS schemes suffer from many problems which become dominant at low speed including sensitivity to machine parameter variation, pure integration effects, inverter nonlinearity, and the quality of stator voltage and current acquisition [2, 4, 6-9].

Generally, a fixed-gain PI controller is employed in the adaptation mechanism of MRAS schemes to produce the estimated position or speed. This is because of its simple structure and ability to generate a satisfactory performance over a wide range of speeds. However, at low speeds, inverter nonlinearities and machine parameter variation become more dominant. As a result, the fixed gain PI may not be able to maintain the system stability or at least to provide the required performance. Moreover, tuning of these PI gains is not an easy task and little effort has been devoted in the literature to address this problem. Various solutions to offer alternative approaches to the design of the adaptation mechanism for MRAS estimators have been discussed in the literature. These solutions have focused on replacing the conventional fixed-gain PI adaption mechanism with more advanced algorithms [10-12]. Replacing the PI adaption mechanism by a Sliding Mode (SM) algorithm was suggested in [10, 12]. Although this scheme is shown to improve the estimator dynamic response, it causes a considerable amount of chattering in the estimated speed signal, and a low pass filter is needed to smooth out the estimated rotor speed. In [11], another solution was proposed where the PI controller is replaced by a fuzzy logic (FL) based adaption mechanism. This scheme shows improvement in the estimator dynamic response, but the computational complexity of the FL controller is the main drawback of this scheme.

Over the last few years, interest has grown in the use of predictive control techniques with sensorless applications. In [13-16] predictive control is applied to permanent magnet sensorless motor drives, and in [17] a predictive torque control with sliding mode feedback is used with a sensorless IM drive. A speed sensorless control system for an IM with a predictive current controller has been proposed in [18], where it has been claimed that this combination can improve the system robustness against motor parameter variations. A new speed and rotor flux linear multivariable generalized predictive control has been introduced in [19] where both the flux and speed observer are included in the proposed scheme. In [20] an encoderless predictive torque control is proposed with a

Manuscript received June 4, 2015; revised August 9, 2015 and November 11, 2015. Accepted for publication January 9, 2016

Y. B. Zbede and D. J. Atkinson are with the School of Electrical and Electronic Engineering, Newcastle University, Newcastle upon Tyne NE1 7RU, U.K. (e-mails: y.zbede@ncl.ac.uk; dave.atkinson@ncl.ac.uk).

S. M. Gadoue is with the School of Electrical and Electronic Engineering, Newcastle University, Newcastle upon Tyne NE1 7RU, U.K., and also with the Department of Electrical Engineering, Faculty of Engineering, Alexandria University, Alexandria 21544, Egypt (email: shady.gadoue@ncl.ac.uk).

rotor flux model reference adaptive system estimator to reduce the system cost. A prediction error method-based self-commissioning scheme for an IM sensorless drive is proposed in [21] and according to the authors; this scheme lowers the influence of measurement noise notably. However, in all the aforementioned publications, the prediction principle was applied on the controller side of the drive, and none of the cases considered introducing the prediction principle into the design of the speed estimator itself.

Generally, Model Predictive Controllers (MPC) can be classified into classical MPC and Finite Control Set-MPC (FCS-MPC) [22]. In classical MPC, the controller generates a continuous voltage vector and a modulator is used to apply this voltage to the inverter, whereas in FCS-MPC the controller directly produces a switching state of the inverter [23]. FCS-MPC has increasingly gained popularity and has been applied in many different applications because of its simplicity, compact design and flexibility to include any performance specifications [24-31]. For example in [31], an FSC-MPC was applied to drive an IM fed by a matrix converter to increase the system efficiency, and in [30] current control of a five-phase IM is applied based on the FCS-MPC control principle.

In this paper a novel MRAS speed estimator for sensorless vector control IM drives is introduced to solve the problems associated with the adaption mechanism design. The FCS-MPC control concept is incorporated in the estimator design. In this scheme, the adaptation mechanism is based on solving an optimization problem with the objective of minimizing the speed tuning error signal of the MRAS estimator over a finite number of rotor position angles. A rotor position search algorithm is developed to ensure that the optimal position is obtained at each sampling time. The computational complexity of the proposed scheme is evaluated and a modified method is employed to reduce its execution time to make it suitable for practical implementation. The performance of the proposed predictive estimator is experimentally tested using a 2.2kW IM drive which employs FOC as the motor control strategy. A detailed comparison between the proposed scheme and the classical rotor flux MRAS estimator has been carried out. Results show the superior performance of the proposed scheme at different low speed operating conditions including regeneration and improved robustness against motor parameter variations.

II. Classical Rotor Flux MRAS Estimator

The classical rotor flux based MRAS estimator shown in Fig.1 was first introduced by *Schauder* [6]. It mainly consists of two mathematical models, the reference and adaptive models, and an adaptation mechanism to produce the estimated speed. This scheme is one of the most common rotor speed estimators and many attempts to improve its performance can be found in the literature.

The reference model represents the stator voltage equation in the stator reference frame which can be written as:

$$v_{s\alpha} = R_s \cdot i_{s\alpha} + \sigma L_s \frac{di_{s\alpha}}{dt} + \frac{L_m}{L_r} \cdot \frac{d\psi_{r\alpha}}{dt}$$

$$v_{s\beta} = R_s \cdot i_{s\beta} + \sigma L_s \frac{di_{s\beta}}{dt} + \frac{L_m}{L_r} \cdot \frac{d\psi_{r\beta}}{dt} \qquad (1)$$

where $v_{s\alpha}$, $v_{s\beta}$ are the stator voltage components, $i_{s\alpha}$, $i_{s\beta}$ are the stator current components, $\psi_{s\alpha}$, $\psi_{s\beta}$ are the reference rotor flux linkage components all expressed in the stationary reference frame. L_m is the machine mutual inductance, R_s is the stator resistance, L_s is the stator self-inductance, L_r is the rotor self-inductance and σ is the leakage coefficient given by: $\sigma = 1 - L_m^2/(L_s L_r)$.

The adaptive model represents the rotor voltage equation of the IM in the stator reference frame which can be written as:

$$0 = \frac{1}{T_r}\hat{\psi}_{r\alpha} - \frac{L_m}{T_r} i_{s\alpha} + \frac{d\hat{\psi}_{r\alpha}}{dt} + \hat{\omega}_r \hat{\psi}_{r\alpha}$$

$$0 = \frac{1}{T_r}\hat{\psi}_{r\beta} - \frac{L_m}{T_r} i_{s\beta} + \frac{d\hat{\psi}_{r\beta}}{dt} + \hat{\omega}_r \hat{\psi}_{r\beta} \qquad (2)$$

where T_r is the rotor time constant, $\hat{\omega}_r$ is the estimated rotor speed, $\hat{\psi}_{r\alpha}$ and $\hat{\psi}_{r\beta}$ the adaptive rotor flux linkage components in stationary reference frame.

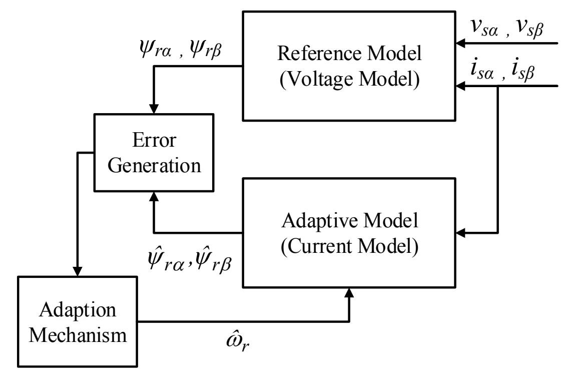

Fig.1 Rotor Flux MRAS structure

The cross coupling presence of the speed dependent components in the adaptive model (2) can lead to an instability issue [32]. Therefore it is common for the rotor flux equation represented in the rotor reference frame to be used:

$$\hat{\psi}_{rd} = \frac{L_m}{1 + T_r \cdot s} i_{sd}$$

$$\hat{\psi}_{rq} = \frac{L_m}{1 + T_r \cdot s} i_{sq} \qquad (3)$$

where i_{sd},i_{sd} are the stator current components, $\hat{\psi}_{rd}$,$\hat{\psi}_{rq}$ are the rotor flux components all expressed in the rotor reference frame. The implementation of the rotor frame based flux model is shown in Fig.2.

The adaption mechanism design is based mainly on the hyperstability theory [2], and as a result of applying this theory, the speed tuning error signal ε can be written as:

$$\varepsilon = \hat{\psi}_{r\alpha}\psi_{r\beta} - \hat{\psi}_{r\beta}\psi_{r\alpha} \qquad (4)$$

A PI controller is used to minimize this error, which in turn generates the estimated speed at its output.

$$\hat{\omega}_r = (K_p + \frac{K_i}{s})\varepsilon \qquad (5)$$

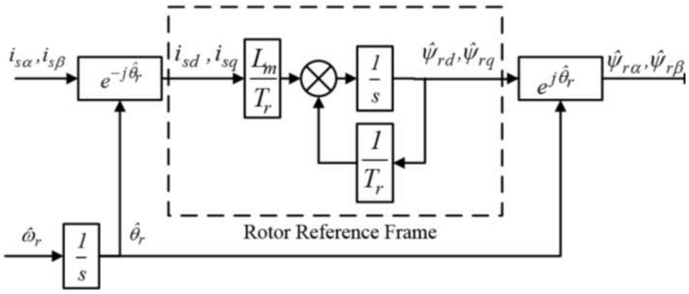

Fig.2 The adaptive model expressed in the rotor reference frame

III. The Proposed Predictive MRAS Estimator

The principle of the proposed predictive MRAS estimator is derived from the Finite Control Set-Model Predictive Controllers (FCS-MPC) concept. In contrast to the conventional model predictive controllers, FCS considers the discrete nature of the inverter in solving the control optimization problem. The cost function is evaluated at each single switching state of the inverter, and the state with the minimum cost function is chosen to be applied in the next sampling instant [33]. This method therefore has the advantages of both simplicity and design flexibility making it attractive to electric drives applications [23].

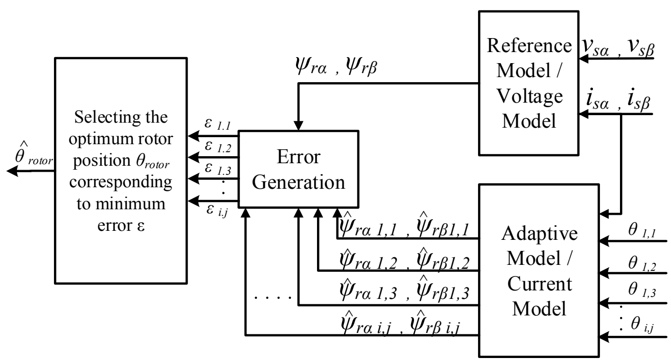

Fig.3 Block diagram of the proposed MRAS estimator

The FCS-MPC approach is applied in this paper to design the adaptation mechanism in MRAS speed estimators. An optimization problem is formulated to find the rotor position in order to minimize a cost function, which is the speed tuning signal ε (4) in the case of the MRAS estimator.

In contrast to the FCS-MPC, the rotor position, which varies continuously between 0 and 360º, does not have the same discrete nature as the inverter output. Therefore a search method is to be applied to discretize the rotor position into a finite number of positions to allow evaluating the cost function at each of these discrete positions. This search is performed within an iteration based process. The block diagram of the proposed predictive MRAS estimator is shown in Fig.3. The flow chart of the proposed search algorithm is shown in Fig.4. The algorithm starts by calculating the reference model outputs $\psi_{r\alpha}$, $\psi_{r\beta}$ from the stator voltages and currents. The discretization of the rotor position begins by starting from an initial base angle $\theta_{base,0}$ and then displacing this angle by a displacement ($\Delta\theta_i$) which is calculated as follow:

$$\Delta\theta_i = 45^o \cdot 2^{-i} \tag{6}$$

where i is the order of the current iteration.

The displacement of the base angle θ_{base} within each iteration is carried out to get eight discrete rotor positions as follow:

$$\theta_{i,j} = \theta_{base} + \Delta\theta_i.(j-4) \tag{7}$$

where j is the order of the displacement.

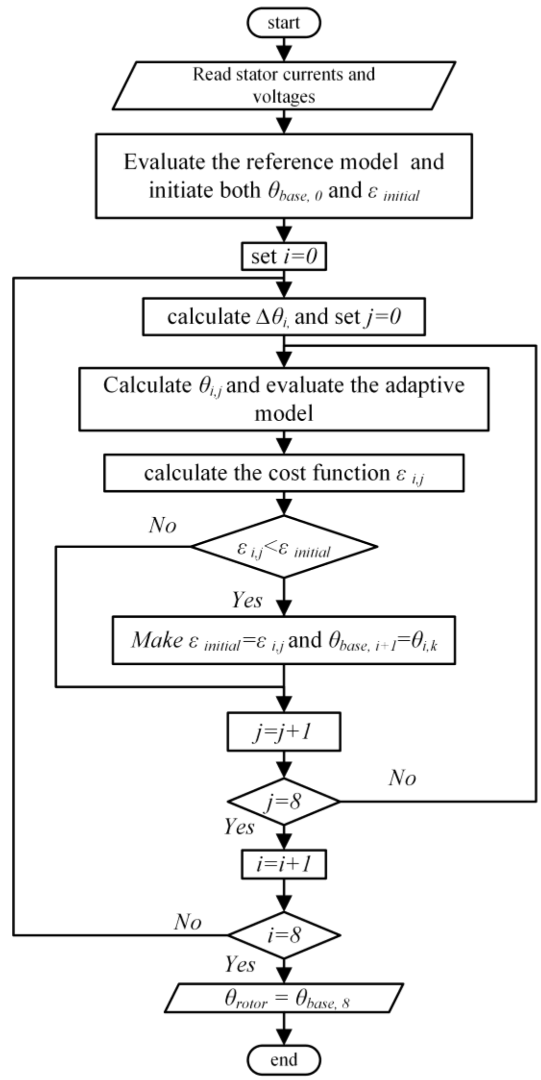

Fig.4 Flowchart of the proposed rotor position search algorithm

In the initial iteration (i=0), the base angle θ_{base} is chosen to be 0° with $\Delta\theta=45^o$ according to (6). Applying (7) will produce eight discrete positions: 0º, 45º, 90º, 135º, 180º, -45º, -90º, -135º. Each of these discrete positions ($\theta_{i,j}$) is used to calculate the adaptive model outputs corresponding to each individual position ($\hat{\psi}_{r\alpha_{i,j}}$ and $\hat{\psi}_{r\beta_{i,j}}$). Consequently the cost function, $\varepsilon_{i,j}$ in (4), is calculated for each position as follows:

$$\varepsilon_{i,j} = \hat{\psi}_{r\alpha_{i,j}} \psi_{r\beta} - \hat{\psi}_{r\beta_{i,j}} \psi_{r\alpha} \tag{8}$$

This leads to eight different cost functions corresponding to each of these angles. The angle corresponding to the minimum cost function of the eight positions is chosen as the base or starting point $\theta_{base,1}$ for the next iteration.

At the next iteration ($i=1$), the angle displacement is decreased to $\Delta\theta_1$=45º×2^{-1}=22.5º, which increases the search accuracy by a factor of 2. The search then starts again from the new base angle $\theta_{base,1}$ to find the angle that generates the minimum cost function in the second iteration. Fig.5 shows the initial and first steps of the search algorithm.

After each iteration, the search algorithm gets closer to the optimal solution, and by the end of the 8th iteration (i=7 and $\Delta\theta_7=0.35°$), the optimal rotor position can be found with 0.35º accuracy. Therefore, by running this algorithm, it can be assured that the optimal rotor position, which produces the minimum cost function throughout the search space, is selected as the output of the estimator.

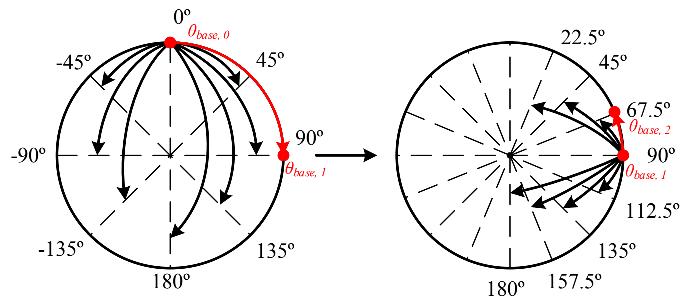

Fig.5 Schematic representation of the first two steps of the proposed search algorithm. (a) Initial iteration. (b) First iteration.

As described previously, the output of the proposed scheme is the rotor position, and to extract the speed signal the following procedure is applied:

The change in rotor position over the last sampling period is calculated from:

$$\Delta\theta = \theta_{rotor}(k) - \theta_{rotor}(k-1) \quad (9)$$

where k is the current time sample.

This change is recorded over 200 samples and the average value is obtained by applying:

$$\Delta\theta_{ave} = \frac{1}{200}\sum_{n=1}^{200}\Delta\theta_n \quad (10)$$

The speed is finally found by dividing the average by the sampling period, the conversion to rad/sec is considered here also.

$$N = \frac{2\pi}{60}\cdot\frac{\Delta\theta_{average}}{T_s} \quad (11)$$

where N is the rotor speed in rpm.

A drawback of the proposed method is the high computational effort required to run the search algorithm eight times in each sampling period. However, the rotor position, as a mechanical variable, changes relatively slowly and hence it does not vary significantly between two time samples. Therefore, instead of initiating the search algorithm in each sampling period with zero angle ($\theta_{base,0}=0$), it can be initialized by the output of the algorithm in the last sampling instant $\theta_{base,0}=\theta_{rotor}(k-1)$. As a result, the number of the iterations required by the search algorithm to find the optimal solution can be significantly reduced as the search is performed only around the previous rotor position. This simplified scheme is referred to as "modified-predictive".

Experimentally, it was found that only the last iteration loop (i=7) is required to find the rotor position using the modified-predictive scheme without affecting the estimation accuracy. This significantly reduces the execution time of the proposed scheme from $103\ \mu s$ to $39\ \mu s$. For comparison purpose, Table I shows the execution times for the two versions of the proposed predictive scheme in addition to the PI-based classical MRAS observer. It should be mentioned here that these times are specific for the TMS320F28335 floating point microcontroller used in the experiments and it can be further reduced if a faster microcontroller is applied. From now on the term "predictive estimator" will be used to refer to the modified scheme with the reduced execution time.

TABLE I
EXECUTION TIME OF THE DIFFERENT ESTIMATORS

Symbol	EXECUTION TIME
PI	$14\ \mu s$
Predictive	$103\ \mu s$
Modified Predictive	$39\ \mu s$

The proposed predictive scheme applies an iterative search method to find the rotor position. This is fundamentally different from other MRAS estimators available in the literature, such as those using PI, sliding mode and fuzzy logic adaptation mechanisms. The proposed method does not require any gain tuning like the aforementioned schemes which make the design of the estimator much simpler and ensure the optimum operation of the estimator at all operating speeds. Application of the proposed scheme always ensures that the speed tuning signal is driven to almost zero in each sampling period. The scheme is capable of achieving minimum error in one sampling time following any disturbance. This results in the proposed scheme having a significant advantage over other approaches.

IV. THE EXPERIMENTAL SYSTEM

The experimental platform used to validate the proposed estimator consists of a 2.2kW, 380V, star-connected, 4-pole, three-phase squirrel cage, IM. The motor is loaded by a 4.19kW, 380V, 8-pole, 2000RPM permanent magnet synchronous machine driven by a Unidrive SP controller manufactured by Control Techniques. The load machine allows independent control of the load torque.

The AC drive consists of a three-phase diode bridge rectifier, and an IGBT-based, three-phase bridge inverter.

To control the AC drive, a TMS320F28335 floating-point microcontroller is used. The control algorithm, based on FOC scheme, is written in C-code and is developed using Code Composer Studio CCS5.5 software. The inverter switching frequency is 10 kHz with a deadtime period of 1 μs and the FOC algorithm is executed with the same sampling frequency.

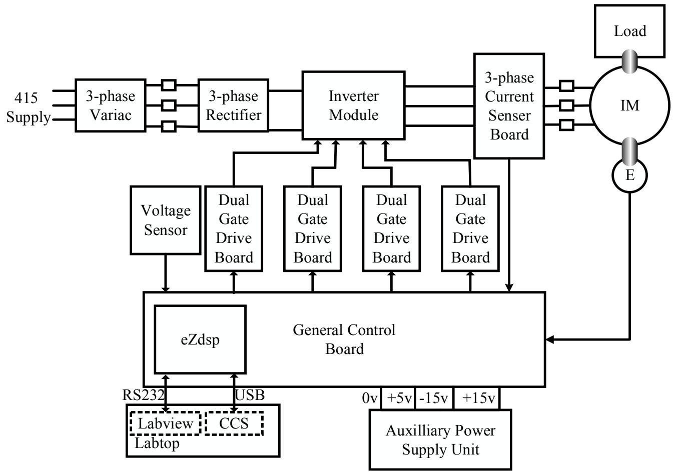

Fig.6 The experimental platform

A 16384 pulses/revolution R1120 Gurley incremental optical encoder is used to measure the actual motor speed, and three CAS-15NP hall-effect current sensors are used to measure the motor phase currents. In addition, an LV25-P voltage sensor is applied to monitor the DC-link voltage.

In order to practically implement both MRAS schemes, the integrator in the reference model was replaced by a low-pass filter with a cut-off frequency of 2Hz to minimise drift and initial condition problems associated with pure integration. As the reference voltage signals available in the controller unit are used in the reference model (1), a compensation for the inverter nonlinearity [34] and a dead band compensator,[35], are implemented.

V. Experimental Results

To evaluate the comparative performance of the proposed predictive MRAS estimator and the classical rotor flux-based MRAS scheme, extensive tests, in both open-loop estimation and sensorless operation modes, are carried out using FOC scheme as the IM control strategy.

A. Open-loop Estimator Operation

During open-loop estimator operation, the FOC scheme obtains its speed signal from the shaft encoder. The PI controller gains of the classical rotor flux-based MRAS are set to K_p=300 and K_i=*8000* which are tuned using trial-error method to obtain the optimal dynamic performance.

Figs.7-9 show the classical and predictive MRAS estimator performance for 75% load rejection at 1.33% of the rated speed (20rpm). The predictive MRAS shows superiority in comparison with the classical MRAS. The oscillation in the estimated speed is reduced significantly and the speed tuning signal is kept below 0.02 even during the transient operation whereas it reaches 0.1 in the classical MRAS, which is 5 times greater. This means that the predictive estimator provides better tracking between the reference and the adaptive models at all the different operation conditions. The frequency spectrum of the estimated rotor speed signal shows that the harmonic content has been reduced significantly in the predictive estimator. For example, the 17Hz component has been reduced from 0.028 per unit to 0.009 per unit, which is a reduction of 67.8%.

Figs.10-11 show the classical and predictive MRAS performance when 63% of the rated load is applied and the speed reference is changed from 6.6% (100rpm) to -6.6% (-100 rpm) of the rated speed in 8 steps, including zero speed and regeneration operation. During the first half of the experiment, the load is applied to oppose the rotation which means that the machine is operating in the motoring mode (positive speed and positive torque), whereas the torque is supporting the speed over the second half and the motor is operating in the regenerating mode (negative speed and positive torque). From the results it can be seen that the predictive estimator can produce speed estimation with a better quality in terms of reduced oscillations at all the different speeds including zero speed. The speed tuning signal remains less than 0.011 during all transient and steady state conditions, while it reaches 0.055 in the classical MRAS. During the regeneration region the predictive controller provides a better performance with less steady state error and oscillations.

To test the proposed scheme's robustness against motor parameter variations, two experimental tests have been carried out. Within the first test, Fig.12.a, a 50% step change has been applied to the rotor resistance R_r in the estimator model while the machine was running at 300rpm and full load. It can be noticed from the figure that the predictive MRAS estimator is less affected by the rotor resistance change with 14 rpm initial undershoot and 0.15s recovery time compared to 19 rpm initial undershoot and 0.45s recovery time for the classical MRAS. In the second test, Fig.12.b, a step change of 20% has been applied to the mutual inductance L_m in the estimator model. It can be observed that the predictive MRAS scheme shows better performance with less oscillation during transients compared to the classical MRAS. In the two tests, the proposed scheme shows better steady-state rotor speed estimation with less noise level. This improvement in robustness against motor parameter variations is mainly due to the replacement of the PI controller in the adaptation mechanism by a search-based optimization algorithm. It is well reported in the literature that fixed-gain PI controllers are generally not robust to changes in system parameters [36].

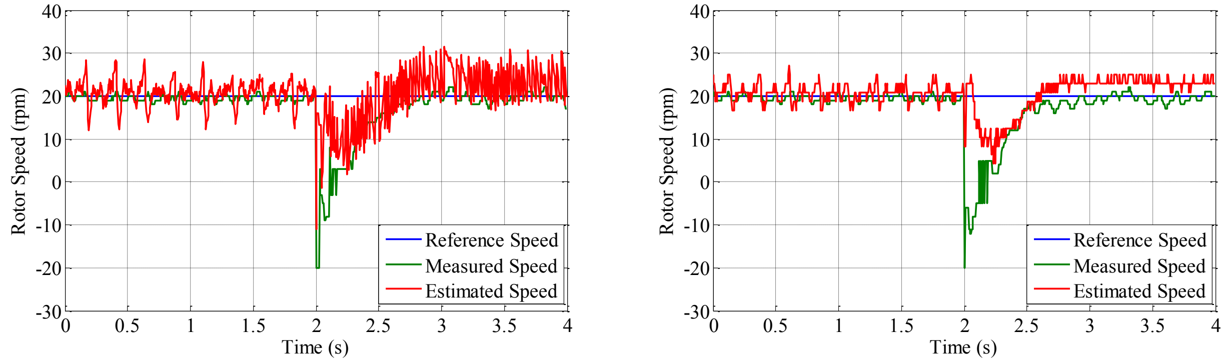

(a) (b)

Fig.7 Open loop estimation, 20 rpm and 75% load, rotor speed (a) Classical MRAS (b) Predictive MRAS

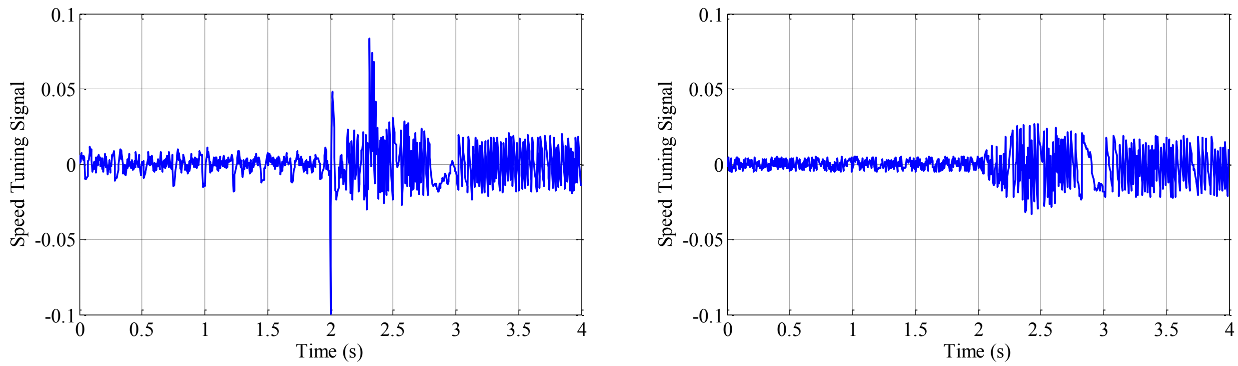

(a) (b)

Fig.8 Open loop estimation 20 rpm and 75% load, speed tuning signal (a) Classical MRAS (b) Predictive MRAS

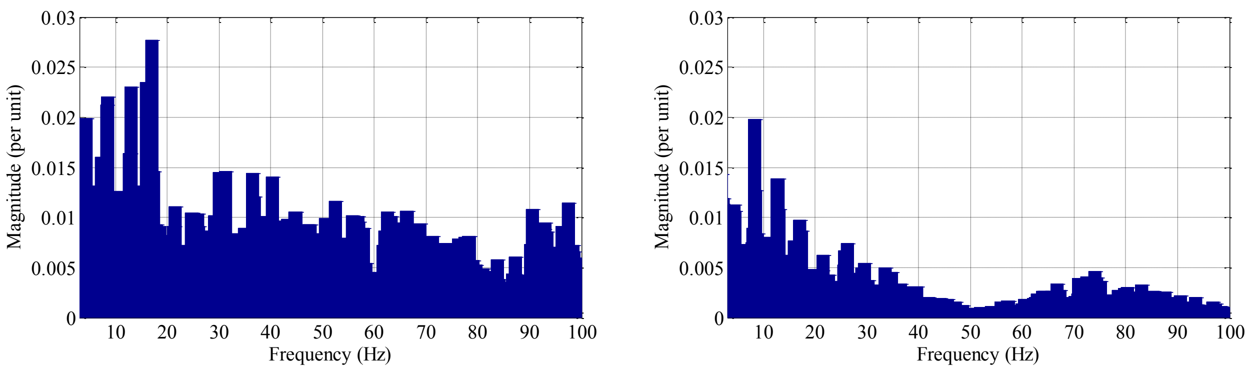

(a) (b)

Fig.9 Open loop estimation, 20 rpm and 75% load, estimated speed frequency spectrum (a) Classical MRAS (b) Predictive MRAS

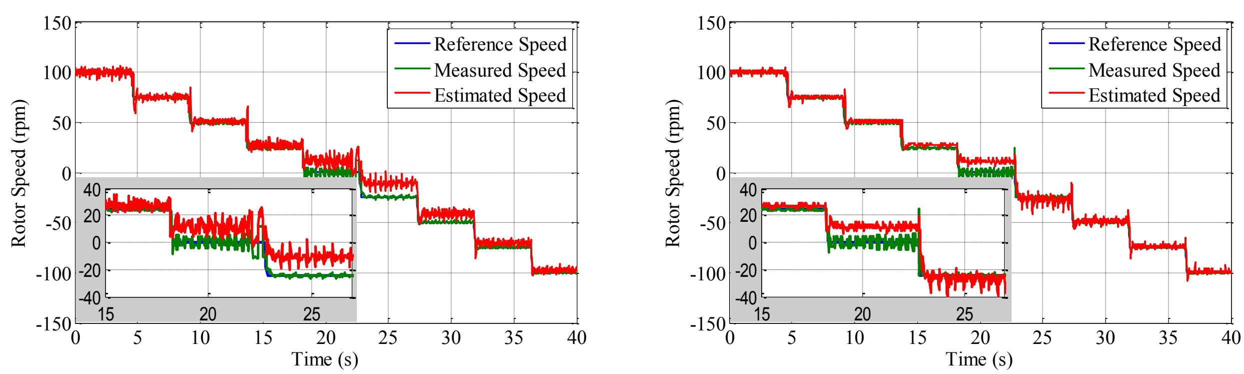

(a) (b)

Fig.10 Open loop estimation 63% load, low speed motoring and regenerating operation, rotor speed (a) Classical MRAS (b) Predictive MRAS

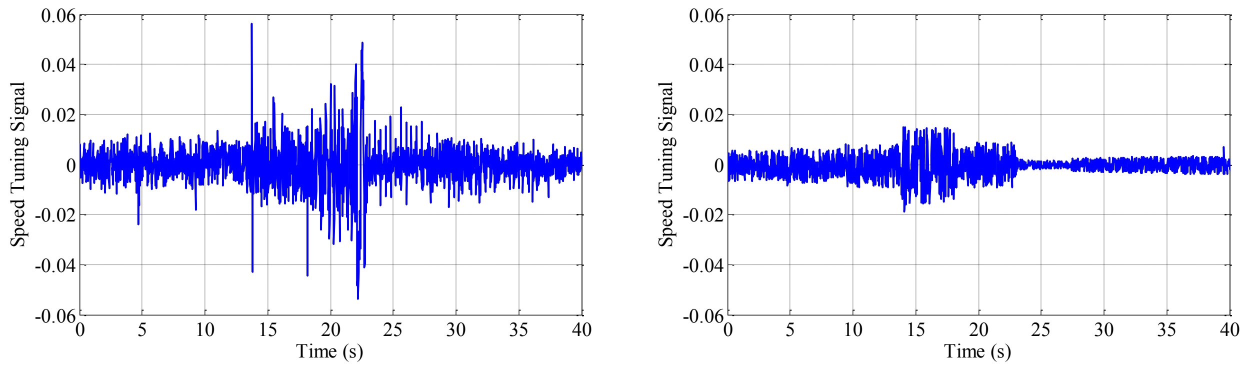

(a) (b)

Fig.11 Open loop estimation, 63% load, low speed motoring and regenerating operation, speed tuning signal (a) Classical MRAS (b) Predictive MRAS

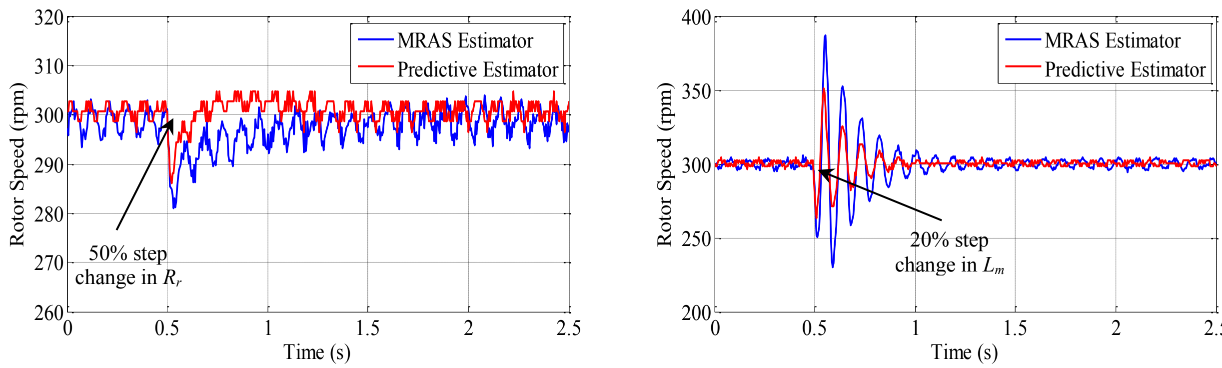

(a) (b)

Fig.12 Open loop estimation, 300 rpm and full load, effect of motor parameters variation. (a) 50% Change in R_r (b) 20% Change in L_m

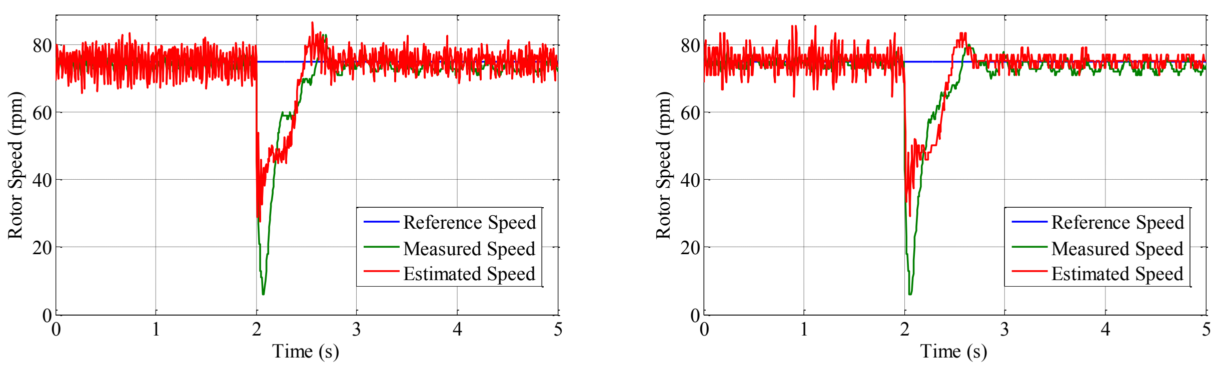

(a) (b)

Fig.13 Sensorless performance, 75 rpm and 75% Load, rotor speed (a) Classical MRAS (b) Predictive MRAS

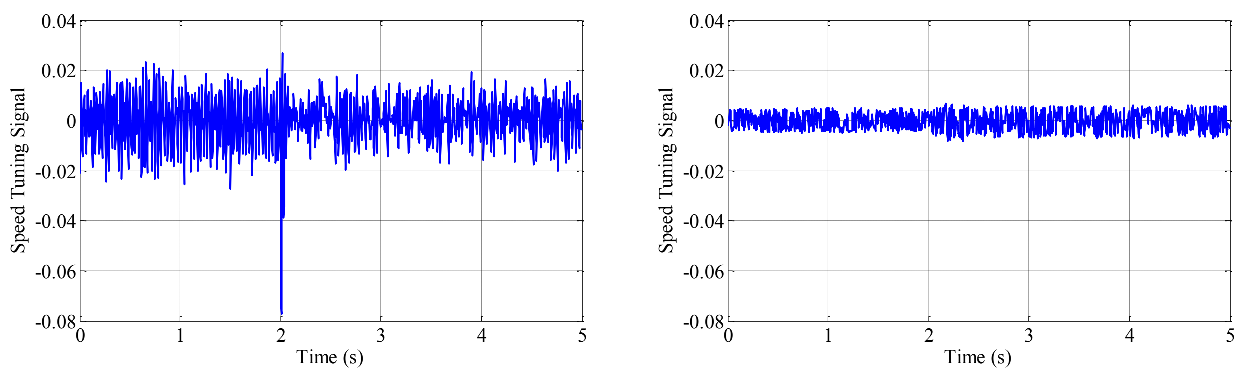

(a) (b)

Fig.14 Sensorless performance, 75 rpm and 75% Load, speed tuning signal. (a) Classical MRAS (b) Predictive MRAS

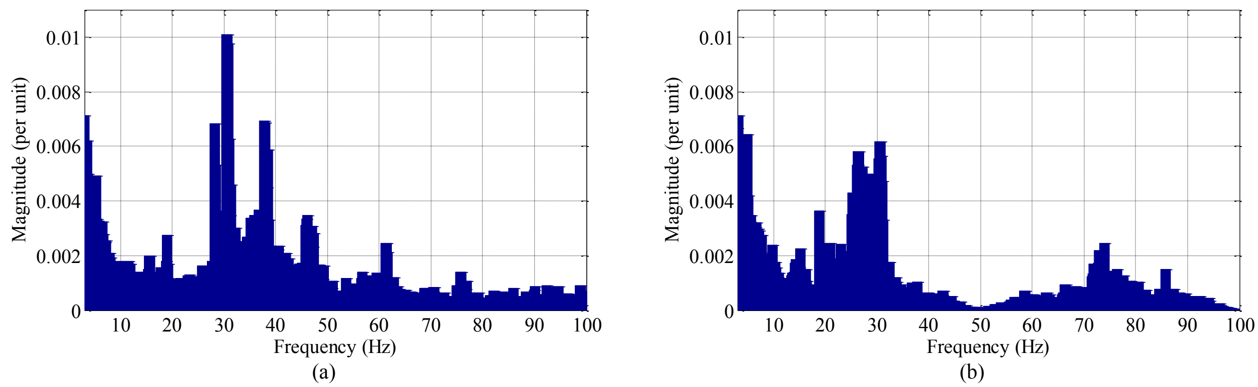

Fig.15 Sensorless performance,75 rpm and 75% Load, estimated speed frequency spectrum. (a) Classical MRAS (b) Predictive MRAS

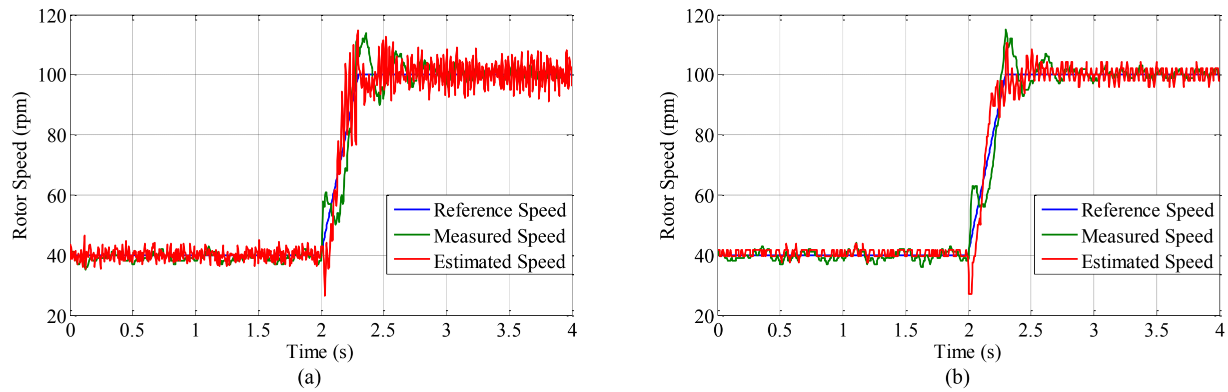

Fig.16 Sensorless performance, reference speed change from 40 to 100 rpm at full load, rotor speed (a) Classical MRAS (b) Predictive MRAS

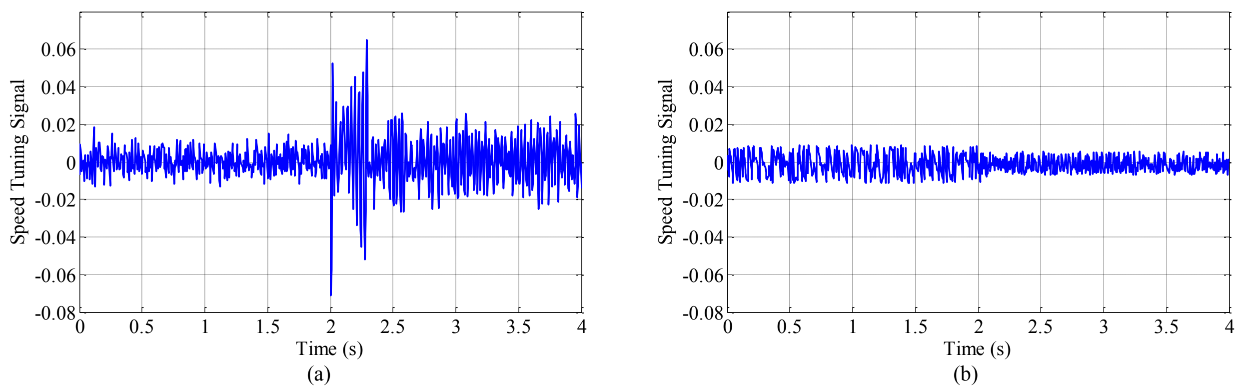

Fig.17 Sensorless performance, reference speed change from 40 to 100 rpm at full load, speed tuning signal (a) Classical MRAS (b) Predictive MRAS

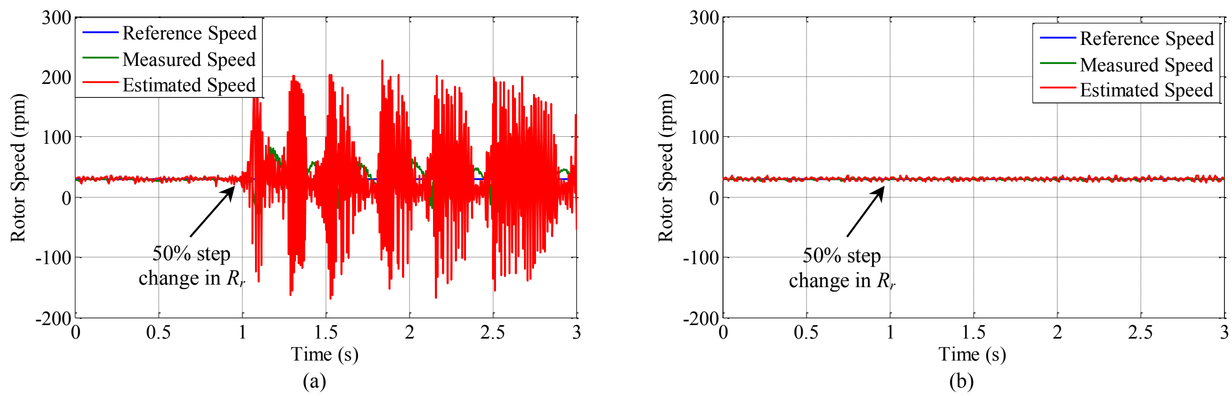

Fig.18 Sensorless performance, the effect of rotor resistance change (a) Classical MRAS (b) Predictive MRAS

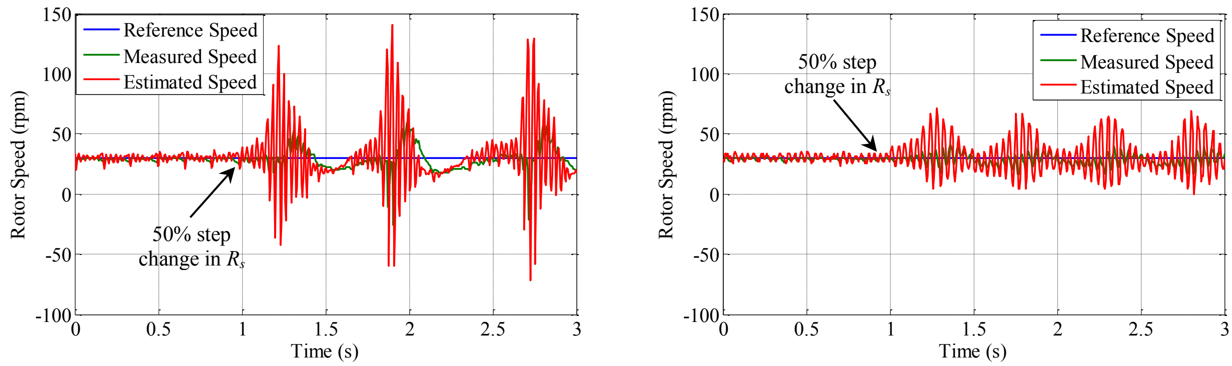

(a) (b)

Fig.19 Sensorless performance, the effect of stator resistance change (a) Classical MRAS (b) Predictive MRAS

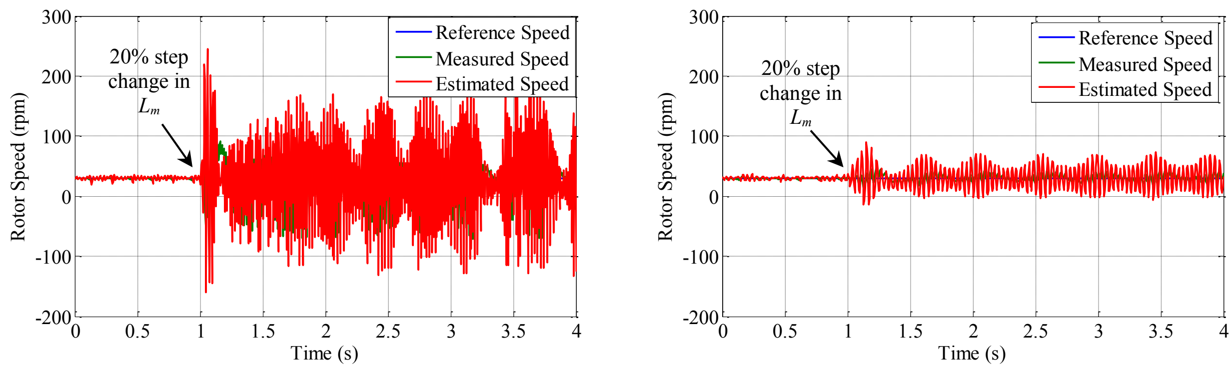

(a) (b)

Fig.20 Sensorless performance, the effect of mutual inductance change (a) Classical MRAS (b) Predictive MRAS

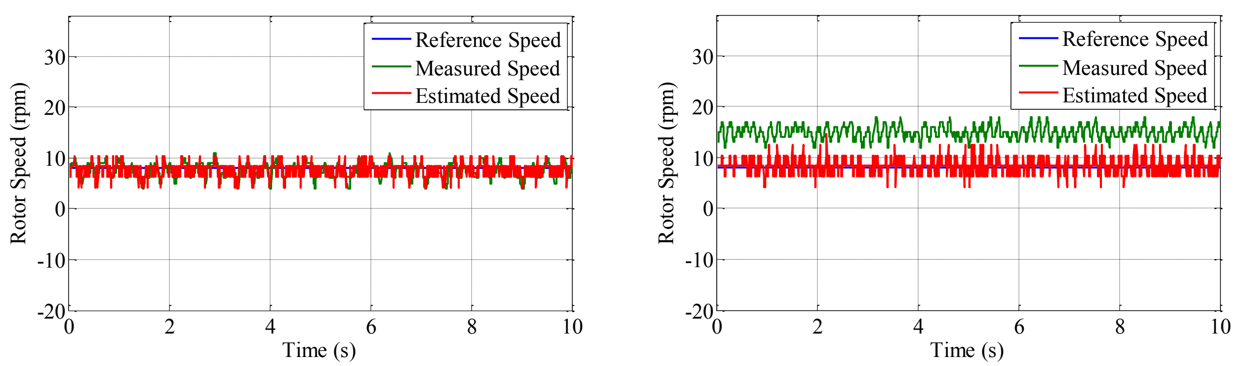

(a) (b)

Fig.21 Sensorless performance at minimum stable speed, Predictive MRAS estimator, (a) No-load (b) Full-load

B. Sensorless Operation

In this operation mode, the FOC scheme is driven by the estimated speed. The performance of both estimators is tested at different speeds and load conditions.

Figs.13-15, show the sensorless operation of both schemes when the drive is subjected to 75% of the rated load at 5% of the rated speed (75 rpm). Once again the predictive MRAS estimator shows a better performance by reducing the oscillation in the estimated speed before and after applying the load, and this improvement appears more clearly in the frequency spectrum of Fig.15. From Fig.14 it can be also noticed that the predictive estimator can produce better tracking between the adaptive and the reference model by keeping the speed tuning signal as small as 0.009 at all the operation points whereas it reaches to 0.08 in the classical estimator when the load is applied.

In Figs.16-17, the speed reference is changed from 2.6% (40rpm) to 6.6% (100rpm) of the rated speed, when rated torque is applied. At both speeds the new estimator shows a better performance when comparing the oscillations in the estimated speeds and speed tuning signals.

In comparison with sliding mode-MRAS estimator results presented in [10], this estimator offers much higher quality speed estimation with a reduced level of noise. Furthermore, no low pass filter is needed to smooth out the estimated rotor speed. The proposed scheme is also less computationally demanding when compared to a rule-based fuzzy logic based-scheme.

To further validate the robustness of the proposed scheme against motor parameter variations, additional experimental tests have been carried when the machine was running at 30 rpm and no-load in sensorless mode of operation. In the first test, Fig. 18, a 50% step change has been applied to the rotor resistance R_r in the estimator model. It is evident from Fig. 18 that the predictive MRAS estimator is far less affected by the rotor resistance change, while the drive system loses stability in the case of the classical MRAS for the same level of R_r change. In the second test, Fig. 19, a step change of 50% has been applied to the stator resistance R_s in the estimator model. It can be observed that the predictive MRAS scheme shows better performance with less oscillation in both the estimated and measured speeds. In the third test, Fig. 20, a step change of 20% has been applied to the mutual inductance L_m in the estimator model. Fig. 20 shows that the classical MRAS scheme has completely lost its stability after applying the change while the proposed predictive MRAS has shown much better performance.

To determine the minimum operating speed of the predictive MRAS estimator, the reference speed is gradually reduced until the motor loses satisfactory operation. It was found that the minimum speed that can be achieved in the case of the predictive MRAS is 8 rpm compared to 25 rpm for the classical MRAS, a 68% improvement in low speed capability. Fig.21 shows the sensorless operation of the proposed scheme at its minimum speed at both no-load and full-load conditions.

The effect of using the predictive estimator on the speed controller bandwidth has been also tested. As the estimated speed of the proposed scheme is less noisy than the classical MRAS, this allows a further increase the PI gains of the speed control loop which will in-turn increase the maximum bandwidth that can be achieved. Experimentally, it has been found that the maximum bandwidth of the predictive MRAS estimator is 156.68 rad/s compared to 85.63 rad/s for the classical MRAS.

VI. Conclusion

In this paper, a novel predictive MRAS rotor speed estimator is proposed for sensorless IM drives. The new estimator is based on the finite control set-model predictive control principle and applies an optimization approach to minimize the speed tuning error signal of the MRAS scheme. This eliminates the need for a PI controller in the adaptation mechanism. A search algorithm is employed to ensure that optimal rotor position is achieved in each sampling period that minimizes the error signal. A modification has been introduced to the proposed algorithm to reduce its computational complexity compared to conventional PI controller. Detailed experimental tests were carried out to compare the performance of the proposed and the classical rotor flux based MRAS schemes. Results show a better estimation quality of the rotor speed with a significant reduction in steady state oscillations without affecting the dynamic response as a minimum speed tuning signal is ensured in both transient and steady state conditions. Hence a higher maximum bandwidth of the speed control loop was achieved when the proposed estimator is employed. Improved robustness against motor parameter variations was also demonstrated for the proposed scheme.

Appendix

TABLE II: Motor Parameters

Symbol	Quantity	Value
Rs	Stator resistance	2.35 Ω
Rr	Rotor resistance	1.05 Ω
Ls	Stator inductance	0.344209 H
Lr	Rotor Inductance	0.348197 H
Lm	Mutual inductance	0.33209 H
J	Motor inertia	$0.22Kg.m^2$

References

[1] B. Drury, *The Control Techniques Drives and Controls Handbook 2ed*, London, 2009.

[2] P. Vas, *Sensorless Vector and Direct torque control*, New York: Oxford University Press, 1998.

[3] P. L. Jansen, R. D. Lorenz, and D. W. Novotny, "Observer-based direct field orientation: analysis and comparison of alternative methods," *IEEE Trans. Ind. Applicat.,* vol. 30, no. 4, pp. 945-953, 1994.

[4] M. Rashed, and A. F. Stronach, "A stable back-EMF MRAS-based sensorless low-speed induction motor drive insensitive to stator resistance variation," *IEE Proc., Electr. Power Appl.,* vol. 151, no. 6, pp. 685-693, 2004.

[5] R. Blasco-Gimenez, G. M. Asher, M. Sumner *et al.*, "Dynamic performance limitations for MRAS based sensorless induction motor drives. 2. Online parameter tuning and dynamic performance studies," *IEE Proc., Electr. Power Appl.,* vol. 143, no. 2, pp. 123-134, 1996.

[6] C. Schauder, "Adaptive speed identification for vector control of induction motors without rotational transducers," *IEEE Trans. Ind. Applicat.,* vol. 28, no. 5, pp. 1054-1061, 1992.

[7] J. Holtz, and J. Quan, "Drift and parameter compensated flux estimator for persistent zero stator frequency operation of sensorless controlled induction motors," *Industry Applications Conference, 2002. 37th IAS Annual Meeting. Conference Record of the,* vol. 3, pp. 1687-1694 vol.3, 13-18 Oct. 2002, 2002.

[8] L. Zhao, J. Huang, H. Liu *et al.*, "Second-Order Sliding-Mode Observer With Online Parameter Identification for Sensorless Induction Motor Drives," *IEEE Trans. Ind. Electron.,* vol. 61, no. 10, pp. 5280-5289, 2014.

[9] D. P. Marcetic, I. R. Krcmar, M. A. Gecic *et al.*, "Discrete Rotor Flux and Speed Estimators for High-Speed Shaft-Sensorless IM Drives," *IEEE Trans. Ind. Electron.,* vol. 61, no. 6, pp. 3099-3108, 2014.

[10] S. M. Gadoue, D. Giaouris, and J. W. Finch, "MRAS Sensorless Vector Control of an Induction Motor Using New Sliding-Mode and Fuzzy-Logic Adaptation Mechanisms," *IEEE Trans. Energy Convers.,* vol. 25, no. 2, pp. 394-402, 2010.

[11] S. M. Gadoue, D. Giaouris, and J. W. Finch, "A new fuzzy logic based adaptation mechanism for MRAS sensorless vector control induction motor drives," *Power Electron, Machines and Drives, 2008. PEMD 2008. 4th IET Conference on*, pp. 179-183, 2-4 April 2008, 2008.

[12] M. Comanescu, and L. Xu, "Sliding-mode MRAS speed estimators for sensorless vector control of induction Machine," *IEEE Trans. Ind. Electron.,* vol. 53, no. 1, pp. 146-153, 2005.

[13] R. Morales-Caporal, E. Bonilla-Huerta, C. Hernandez *et al.*, "Transducerless Acquisition of the Rotor Position for Predictive Torque Controlled PM Synchronous Machines Based on a DSP-FPGA Digital System," *IEEE Trans. Ind. Inf.,* vol. 9, no. 2, pp. 799-807, 2013.

[14] L. Tong, X. Zou, S. Feng *et al.*, "An SRF-PLL-Based Sensorless Vector Control Using the Predictive Deadbeat Algorithm for the Direct-Driven Permanent Magnet Synchronous Generator," *IEEE Trans. Power Electron.,* vol. 29, no. 6, pp. 2837-2849, 2014.

[15] R. Morales-Caporal, E. Bonilla-Huerta, M. A. Arjona *et al.*, "Sensorless Predictive DTC of a Surface-Mounted Permanent-Magnet Synchronous Machine Based on Its Magnetic Anisotropy," *IEEE Trans. Ind. Electron.,* vol. 60, no. 8, pp. 3016-3024, 2013.

[16] J. L. Chen, and T. H. Liu, "Implementation of a predictive controller for a sensorless interior permanent-magnet synchronous

motor drive system," *IET, Electr. Power Appl.,* vol. 6, no. 8, pp. 513-525, 2012.
[17] S. Alireza Davari, D. A. Khaburi, F. Wang *et al.*, "Using Full Order and Reduced Order Observers for Robust Sensorless Predictive Torque Control of Induction Motors," *IEEE Trans. Power Electron.,* vol. 27, no. 7, pp. 3424-3433, 2012.
[18] J. Guzinski, and H. Abu-Rub, "Speed Sensorless Induction Motor Drive With Predictive Current Controller," *IEEE Trans. Ind. Electron.,* vol. 60, no. 2, pp. 699-709, 2013.
[19] P. Alkorta, O. Barambones, J. A. Cortajarena *et al.*, "Efficient Multivariable Generalized Predictive Control for Sensorless Induction Motor Drives," *IEEE Trans. Ind. Electron.,* vol. 61, no. 9, pp. 5126-5134, 2014.
[20] F. Wang, Z. Chen, P. Stolze *et al.*, "Encoderless Finite-State Predictive Torque Control for Induction Machine With a Compensated MRAS," *IEEE Trans. Ind. Inf.,* vol. 10, no. 2, pp. 1097-1106, 2014.
[21] J. Ruan, and S. Wang, "A Prediction Error Method-Based Self-Commissioning Scheme for Parameter Identification of Induction Motors in Sensorless Drives," *IEEE Trans. Energy Convers.,* vol. 30, no. 1, pp. 384-393, 2015.
[22] A. Linder, and R. Kennel, "Direct model predictive control - a new direct predictive control strategy for electrical drives," *Power Electronics and Applications, 2005 European Conference on*, pp. 10 pp.-P.10, 0-0 0, 2005.
[23] S. Saeidi, and R. Kennel, "A novel algorithm for model predictive control of AC electric drives," *Electric Drives Production Conference (EDPC), 2012 2nd International*, pp. 1-7, 15-18 Oct. 2012, 2012.
[24] S. Kouro, P. Cortes, R. Vargas *et al.*, "Model Predictive Control-A Simple and Powerful Method to Control Power Converters," *IEEE Trans. Ind. Electron.,* vol. 56, no. 6, pp. 1826-1838, 2009.
[25] J. Rodriguez, J. Pontt, C. A. Silva *et al.*, "Predictive Current Control of a Voltage Source Inverter," *IEEE Trans. Ind. Electron.,* vol. 54, no. 1, pp. 495-503, 2007.
[26] P. Cortes, M. P. Kazmierkowski, R. M. Kennel *et al.*, "Predictive Control in Power Electronics and Drives," *IEEE Trans. Ind. Electron.,* vol. 55, no. 12, pp. 4312-4324, 2008.
[27] T. Geyer, G. Papafotiou, and M. Morari, "Model Predictive Direct Torque Control-Part I: Concept, Algorithm, and Analysis," *IEEE Trans. Ind. Electron.,* vol. 56, no. 6, pp. 1894-1905, 2009.
[28] G. Papafotiou, J. Kley, K. G. Papadopoulos *et al.*, "Model Predictive Direct Torque Control-Part II: Implementation and Experimental Evaluation," *IEEE Trans. Ind. Electron.,* vol. 56, no. 6, pp. 1906-1915, 2009.
[29] F. Wang, Z. Zhang, S. Alireza Davari *et al.*, "An Encoderless Predictive Torque Control for an Induction Machine With a Revised Prediction Model and EFOSMO," *IEEE Trans. Ind. Electron.,* vol. 61, no. 12, pp. 6635-6644, 2014.
[30] C. S. Lim, E. Levi, M. Jones *et al.*, "FCS-MPC-Based Current Control of a Five-Phase Induction Motor and its Comparison with PI-PWM Control," *IEEE Trans. Ind. Electron.,* vol. 61, no. 1, pp. 149-163, 2014.
[31] R. Vargas, J. Rodriguez, C. A. Rojas *et al.*, "Predictive Control of an Induction Machine Fed by a Matrix Converter With Increased Efficiency and Reduced Common-Mode Voltage," *IEEE Trans. Energy Convers.,* vol. 29, no. 2, pp. 473-485, 2014.
[32] P. L. Jansen, and R. D. Lorenz, "A physically insightful approach to the design and accuracy assessment of flux observers for field oriented induction machine drives," *Industry Applications Society Annual Meeting, 1992., Conference Record of the 1992 IEEE*, pp. 570-577 vol.1, 4-9 Oct 1992, 1992.
[33] S. A. Davari, D. A. Khaburi, and R. Kennel, "An Improved FCS-MPC Algorithm for an Induction Motor With an Imposed Optimized Weighting Factor," *IEEE Trans. Power Electron.,* vol. 27, no. 3, pp. 1540-1551, 2012.
[34] J. Holtz, and J. Quan, "Sensorless vector control of induction motors at very low speed using a nonlinear inverter model and parameter identification," *IEEE Trans. Ind. Applicat.,* vol. 38, no. 4, pp. 1087-1095, 2002.
[35] S. H. Kim, T. S. Park, J. Y. Yoo *et al.*, "Dead time compensation in a vector-controlled induction machine," *Power Electron Specialists Conference, 1998. PESC 98 Record. 29th Annual IEEE,* vol. 2, pp. 1011-1016 vol.2, 17-22 May 1998, 1998.
[36] Y. N. Lin, and C. L. Chen, "Adaptive pseudoreduced-order flux observer for speed sensorless field-oriented control of IM," *IEEE Trans. Ind. Electron.,* vol. 46, no. 5, pp. 1042-1045, 1999.

Yaman B. Zbede received the B.Sc. degree in electrical engineering from Aleppo University, Aleppo, Syria, in 2009, and the M.Sc. degree in Electrical Power from Newcastle University, Newcastle upon Tyne, U.K., in 2012, where he is currently working toward the Ph.D. degree in electrical engineering.

His main research interest is in the area of electrical machine drives and control.

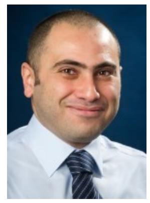

Shady M. Gadoue received the B.Sc. and M.Sc. degrees from Alexandria University, Alexandria, Egypt, in 2000 and 2003, respectively, and the Ph.D. degree from Newcastle University, Newcastle upon Tyne, U.K., in 2009, all in electrical engineering.

From 2009 to 2011, he was an Assistant Professor with the Department of Electrical Engineering, Alexandria University, where he was an Assistant Lecturer from 2000 to 2005. In 2011, he joined the Electrical Power Research Group, Newcastle University, as a Lecturer in Control Systems. His main research interests include control, state and parameter identification, and optimization algorithms applied to energy conversion and motor drives systems.

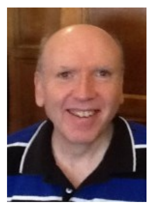

David J. Atkinson obtained his BSc in electrical and electronic engineering from Sunderland Polytechnic, England, in 1978 and his PhD from Newcastle University, England, in 1991. He is a Senior Lecturer in the Electrical Power Research Group at the School of Electrical and Electronic Engineering, Newcastle University, UK. He joined the university in 1987 after 17 years in industry with NEI Reyrolle Ltd and British Gas Corporation. His research interests are focussed on the control of power electronics systems including electric drives and converters for renewable energy systems. Dr Atkinson is a chartered electrical engineer and a recipient of the Power Premium awarded by the Institution of Electrical Engineers (IEE).